

# **Novel phosphorescent iridium(III) complexes containing 2-thienyl quinazoline ligand: synthesis, photophysical properties and theoretical calculation**

Qunbo Mei,<sup>\*,a</sup> Jienna Weng,<sup>a,c</sup> Zhijie Xu,<sup>a</sup> Bihai Tong,<sup>b</sup> Qingfang Hua,<sup>a</sup> Yujie Shi,<sup>a</sup> Juan Song<sup>a</sup> and Wei Huang<sup>\*,a,c</sup>

<sup>a</sup>Key Laboratory for Organic Electronics and Information Displays & Institute of Advanced Materials(IAM), Jiangsu National Synergetic Innovation Center for Advanced Materials (SICAM), Nanjing University of Posts & Telecommunications, 9 Wenyuan Road, Nanjing 210023, China; E-mail: iamqbmei@njupt.edu.cn.

<sup>b</sup>College of Metallurgy and Resources, Anhui University of Technology, Ma'anshan, Anhui 243002, P. R. China;

<sup>c</sup>Key Laboratory of Flexible Electronics (KLOFE) & Institute of Advanced Materials (IAM), Jiangsu National Synergetic Innovation Center for Advanced Materials (SICAM), Nanjing Tech University, 30 South Puzhu Road, Nanjing 211816, China; E-mail: iamwhuang@njupt.edu.cn

## **Contents:**

- 1. Supplementary Figures and Tables**
- 2. Characterizations: <sup>1</sup>H-NMR, <sup>13</sup>C-NMR, and MADIL-TOF-MS spectra**

## 1. Supplementary Figures and Tables

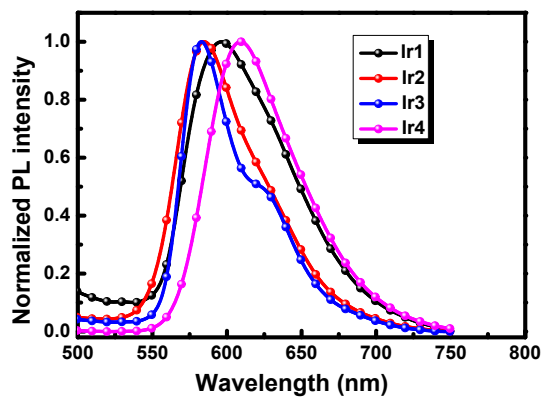


Figure. S1 Photoluminescence spectra of complexes Ir1-Ir4 in 2 wt% PMMA films at room temperature

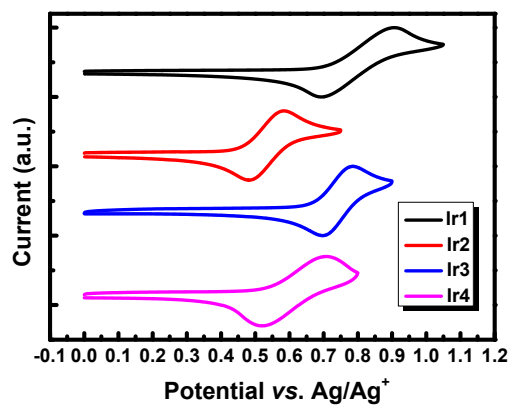


Figure. S2 Cyclic voltammogram of complexes Ir1-Ir4 in deoxygenated DCM solutions at room temperature.

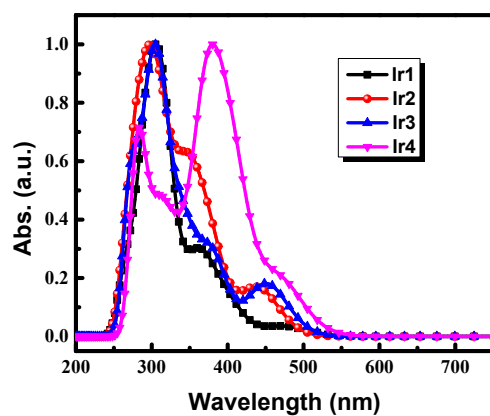
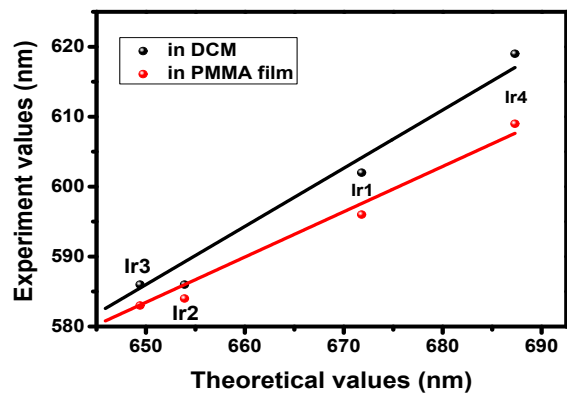


Fig. S3 The simulated absorption spectra of complexes Ir1-Ir4 in DCM.



**Figure. S4** The relationship between the theoretical and experimental values of the maximum phosphorescence emissions.

**Table S1** XRD experimental details

	Ir1	Ir2	Ir3	Ir4
Empirical formula	C <sub>30</sub> H <sub>18</sub> IrN <sub>5</sub> O <sub>2</sub> S <sub>2</sub>	C <sub>40</sub> H <sub>36</sub> IrN <sub>7</sub> O <sub>2</sub> S <sub>2</sub>	C <sub>46</sub> H <sub>34</sub> IrN <sub>5</sub> O <sub>4</sub> S <sub>2</sub>	C <sub>54</sub> H <sub>36</sub> IrN <sub>7</sub> O <sub>2</sub> S <sub>2</sub>
Formula weight	736.81	903.08	977.10	1071.22
Temperature (K)	296	296	296	296
Mo <i>Kα</i> radiation (Å)	λ = 0.71073	λ = 0.71073	λ = 0.71073	λ = 0.71073
Crystal system, space group	Monoclinic, <i>P</i> 2 <sub>1</sub> / <i>n</i>	Triclinic, <i>P</i> $\bar{1}$	Monoclinic, <i>C</i> 2/ <i>c</i>	Monoclinic, <i>P</i> 2 <sub>1</sub> / <i>n</i>
Unit cell dimensions	a = 11.3735 (11) Å α = 90.000 ° b = 12.2222 (11) Å β = 93.385 (1) ° c = 121.987 (2) Å γ = 90.000 °	a = 9.324 (5) Å α = 106.650 (8) ° b = 12.900 (7) Å β = 94.335 (8) ° c = 18.496 (10) Å γ = 91.856 (7) °	a = 27.554 (13) Å α = 90.000 ° b = 17.381 (8) Å β = 122.764 (7) ° c = 23.473 (11) Å γ = 90.000 °	a = 14.908 (3) Å α = 90.000 ° b = 14.425 (3) Å β = 94.332 (4) ° c = 23.345 (5) Å γ = 90.000 °
Volume (Å <sup>3</sup> )	3051.1 (5)	2122 (2)	9453 (8)	4684 Å <sup>3</sup>
<i>Z</i> , Calculated density	4	2	8	4
<i>D<sub>x</sub></i> (Mg/m <sup>3</sup> )	1.604	1.413	1.373	1.421
μ (mm <sup>-1</sup> )	4.55	3.29	2.96	2.80
<i>F</i> (000)	1432	900	3888	2136
Crystal size (mm)	0.26 × 0.24 × 0.22	0.28 × 0.25 × 0.22	0.27 × 0.25 × 0.22	0.26 × 0.24 × 0.22
Theta range for data collection	2.5° - 27.2°	1.2° - 25.0°	1.5° - 25.0°	1.6° - 25.0°
Limiting indices	<i>h</i> = -13 → 11 <i>k</i> = -14 → 14 <i>l</i> = -26 → 20	<i>h</i> = -10 → 11 <i>k</i> = -15 → 15 <i>l</i> = -21 → 12	<i>h</i> = -27 → 32 <i>k</i> = -20 → 20 <i>l</i> = -27 → 22	<i>h</i> = -17 → 12 <i>k</i> = -17 → 17 <i>l</i> = -27 → 27
No. of measured, independent and observed [ <i>I</i> > 2σ( <i>I</i> )] reflections	16314, 5383, 4171	11715, 7432, 6271	25823, 8342, 6649	27285, 8827, 6894
<i>R</i> <sub>int</sub>	0.031	0.026	0.033	0.038
(sinθ/λ) <sub>max</sub> (Å <sup>-1</sup> )	0.595	0.595	0.595	0.595
Refinement method	Refinement on <i>F</i> <sup>2</sup>	Refinement on <i>F</i> <sup>2</sup>	Refinement on <i>F</i> <sup>2</sup>	Refinement on <i>F</i> <sup>2</sup>
Least-squares matrix	full	full	full	full
Data / restraints / parameters	5383 / 0 / 361	7432 / 0 / 469	8342 / 72 / 515	8827 / 48 / 595
Goodness-of-fit on <i>F</i> <sup>2</sup>	1.02	0.97	1.05	1.02
R[ <i>F</i> <sup>2</sup> > 2σ( <i>F</i> <sup>2</sup> )]	0.026	0.031	0.027	0.029
wR( <i>F</i> <sup>2</sup> )	0.060	0.065	0.066	0.072
Δρ <sub>max</sub> , Δρ <sub>min</sub> (e Å <sup>-3</sup> )	0.81, -0.72	0.84, -0.95	0.61, -0.51	1.03, -0.53

**Table S2** Selected bond lengths of complexes **Ir1-Ir4**

<b>Ir1</b>	Bond length (Å)	<b>Ir2</b>	Bond length (Å)	<b>Ir3</b>	Bond length (Å)	<b>Ir4</b>	Bond length (Å)
Ir-C30	2.001(4)	Ir-C15	1.980(4)	Ir-C18	1.983(3)	Ir-C22	1.984(4)
Ir-C21	1.986(4)	Ir-C32	1.966(3)	Ir-C38	1.975(4)	Ir-C46	1.963(4)
Ir-N1	2.049(3)	Ir-N1	2.100(4)	Ir-N3	2.101(3)	Ir-N4	2.083(3)
Ir-N3	2.044(3)	Ir-N4	2.083(4)	Ir-N1	2.077(3)	Ir-N1	2.087(3)
Ir-N5	2.129(3)	Ir-N7	2.150(4)	Ir-N5	2.157(5)	Ir-N7	2.164(3)
Ir-O1	2.148(2)	Ir-O1	2.158(3)	Ir-O3	2.149(4)	Ir-O1	2.138(3)

**Table S3** Selected bond angles of complexes **Ir1-Ir4**

<b>Ir1</b>	Bond angle (°)	<b>Ir2</b>	Bond angle (°)	<b>Ir3</b>	Bond angle (°)	<b>Ir4</b>	Bond angle (°)
C30-Ir-C21	86.9(2)	C15-Ir-C32	92.6(2)	C18-Ir-C38	93.0(2)	C22-Ir-C46	95.3(2)
C30-Ir-N1	80.6(2)	C15-Ir-N1	79.3(1)	C18-Ir-N3	79.5(1)	C22-Ir-N4	79.7(1)
C30-Ir-N3	95.1(1)	C15-Ir-N4	92.7(1)	C18-Ir-N1	93.5(1)	C22-Ir-N1	94.4(1)
C30-Ir-N5	173.6(1)	C15-Ir-N7	171.5(1)	C18-Ir-N5	169.7(2)	C22-Ir-N7	165.8(1)
C30-Ir-O1	98.2(1)	C15-Ir-O1	95.3(1)	C18-Ir-O3	93.2(2)	C22-Ir-O1	90.2(1)
C21-Ir-N1	96.1(1)	C32-Ir-N1	99.0(1)	C38-Ir-N3	94.6(1)	C46-Ir-N4	95.7(1)
C21-Ir-N3	80.0(1)	C32-Ir-N4	79.6(1)	C38-Ir-N1	79.6(1)	C46-Ir-N1	79.7(1)
C21-Ir-N5	98.5(1)	C32-Ir-N7	95.7(1)	C38-Ir-N5	96.5(2)	C46-Ir-N7	98.3(1)
C21-Ir-O1	172.3(1)	C32-Ir-O1	172.0(1)	C38-Ir-O3	173.4(2)	C46-Ir-O1	173.8(1)
N1-Ir-N3	174.4(1)	N1-Ir-N4	171.8(1)	N3-Ir-N1	170.8(1)	N4-Ir-N1	172.2(1)
N1-Ir-N5	95.4(1)	N1-Ir-N7	101.2(1)	N3-Ir-N5	103.5(1)	N4-Ir-N7	103.0(1)
N1-Ir-O1	90.4(1)	N1-Ir-O1	82.9(1)	N3-Ir-O3	84.5(1)	N4-Ir-O1	82.5(1)
N3-Ir-N5	89.2(1)	N4-Ir-N7	87.0(1)	N1-Ir-N5	84.5(1)	N1-Ir-N7	84.0(1)
N3-Ir-O1	93.8(1)	N4-Ir-O1	99.7(1)	N1-Ir-O3	102.1(1)	N1-Ir-O1	102.7(1)
N5-Ir-O1	76.8(1)	N7-Ir-O1	76.3(1)	N5-Ir-O1	77.4(2)	N7-Ir-O1	76.4(1)

**Table S4** Orbital composition analysis for **Ir1–Ir4** at their lowest singlet state ( $S_0$ ) geometries

Complex	Orbital	Ir	C^N (1)				C^N (2)				N^O
			total	QZ	Th	substituent	total	QZ	Th	substituent	
<b>Ir1</b>	LUMO	1.7%	5.5%	3.9%	1.6%	--	91.8%	66.4%	17.0%	--	0.9%
	HOMO	33.0%	35.8%	22.7%	13.1%	--	27.7%	25.4%	10.4%	--	3.6%
<b>Ir2</b>	LUMO+1	2.2%	81.1%	59.6%	13.9%	7.6%	0.7%	0.5%	0.0%	0.2%	16.0%
	LUMO	3.0%	0.4%	0.1%	0.2%	0.0%	95.7%	71.4%	15.8%	8.5%	0.9%
	HOMO	34.7%	32.6%	7.7%	24.8%	0.1%	29.6%	7.1%	22.4%	0.1%	3.1%
	<b>Ir3</b>	LUMO+1	3.3%	89.6%	69.5%	16.3%	3.8%	4.1%	7.9%	20.9%	0.0%
	LUMO	3.5%	4.7%	3.4%	1.1%	0.2%	90.9%	71.2%	19.1%	0.6%	0.9%
	HOMO	34.3%	33.9%	9.0%	24.8%	0.0%	28.9%	3.4%	0.7%	0.0%	3.0%
<b>Ir4</b>	LUMO+1	3.6%	0.8%	0.5	0.3	0.0	94.3%	69.5%	13.8	11.0	1.4%
	LUMO	2.5%	94.5%	72.3	10.7	11.5	0.5%	0.2	0.2	0.0	2.5%
	HOMO	34.5%	30.4%	7.8	22.6	0.0	32.0%	7.8	23.9	0.3	3.1%

**Table S5** Orbital composition analysis for **Ir1–Ir4** at their first excited triplet state ( $T_1$ ) geometries.

Complex	Orbital	Ir	C^N (1)				C^N (2)				N^O
			total	QZ	Th	substituent	total	QZ	Th	substituent	
<b>Ir1</b>	LUMO+4	5.7	71.4	43.7	27.6	--	21.7	13.8	7.8	--	1.2
	LUMO	1.5	96.8	88.4	8.3	--	1.2	0.7	0.5	--	0.5
	HOMO	28.0	48.3	15.8	32.5	--	20.4	5.4	15.0	--	3.4
	HOMO-1	2.5	42.9	18.6	24.3	--	53.4	19.2	34.3	--	1.1
<b>Ir2</b>	LUMO+4	1.9	61.4	44.1	16.1	1.2	34.1	25.6	7.8	0.6	2.6
	LUMO	4.2	91.6	62.4	23.8	5.4	0.5	0.3	0.2	0.0	3.7
	HOMO	28.8	49.1	18.7	30.4	0.1	20.1	5.1	14.9	0.1	1.9
	HOMO-1	20.6	33.5	19.3	10.3	3.9	43.2	20.4	20.5	2.3	2.8
<b>Ir3</b>	LUMO	4.90	5.08	3.34	1.60	0.15	88.84	55.77	30.46	2.62	1.18
	HOMO	29.34	25.65	7.09	18.54	0.02	42.24	15.30	26.92	0.02	2.77
	HOMO-1	17.70	40.74	17.71	22.58	0.45	38.35	21.05	16.61	0.69	3.21
<b>Ir4</b>	LUMO	4.4	0.8	0.4	0.3	0.0	93.9	71.4	14.7	7.9	0.9
	HOMO	30.4	28.6	7.5	20.9	0.1	38.1	12.7	25.4	0.1	2.8
	HOMO-1	12.1	19.0	8.3	6.1	4.6	67.5	18.7	4.4	44.3	1.4
	HOMO-3	2.3	57.5	6.5	19.7	31.4	39.1	14.4	16.8	10.9	1.0

## 2. Characterizations: $^1\text{H}$ -NMR, $^{13}\text{C}$ -NMR, and MADIL-TOF-MS spectra

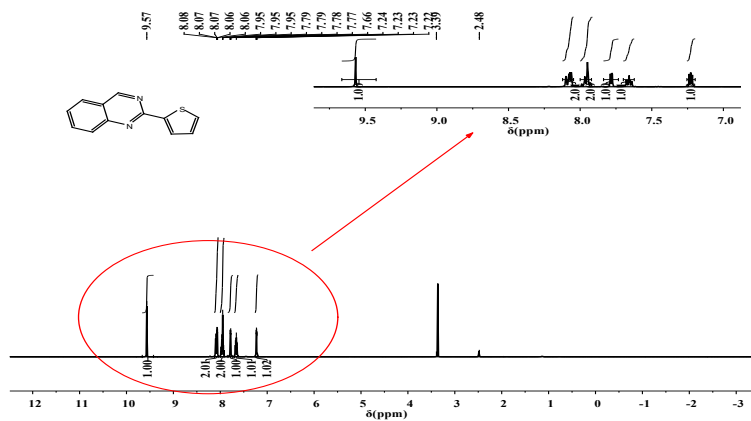


Figure S5.  $^1\text{H}$  NMR of L1 in DMSO

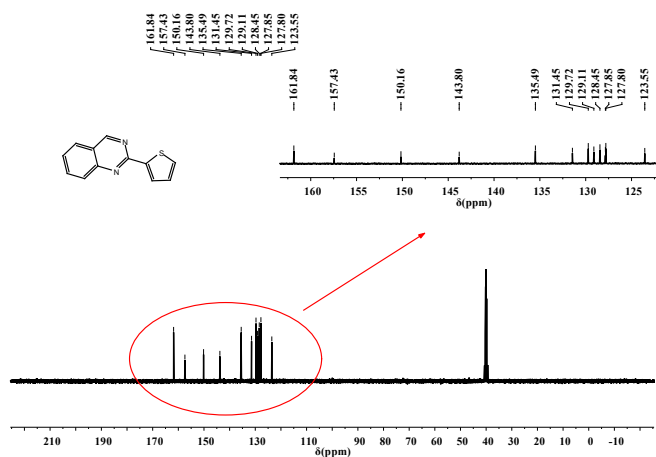


Figure S6.  $^{13}\text{C}$  NMR of L1 in DMSO

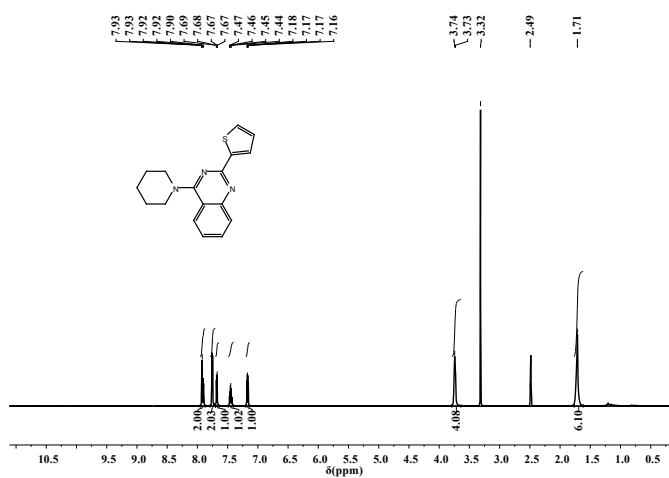


Figure S7.  $^1\text{H}$  NMR of L2 in DMSO





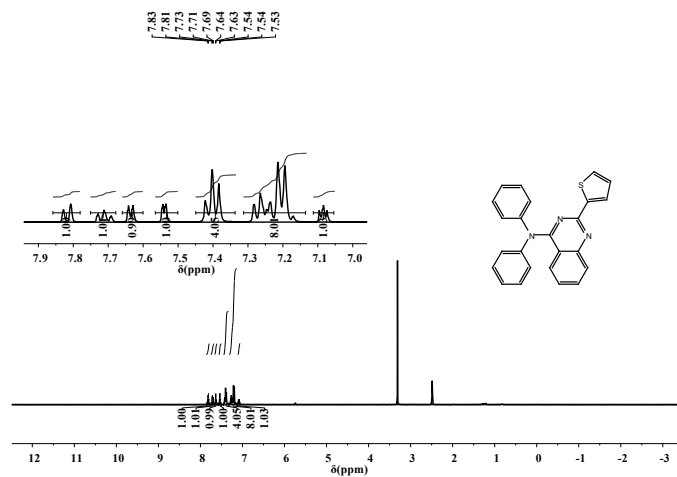


Figure S11. <sup>1</sup>H NMR of L4 in DMSO

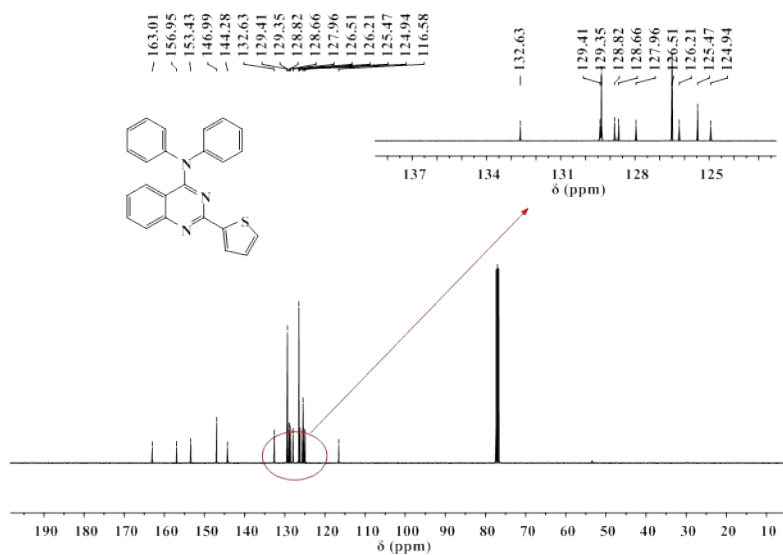


Figure S12. <sup>13</sup>C NMR of L4 in CDCl<sub>3</sub>

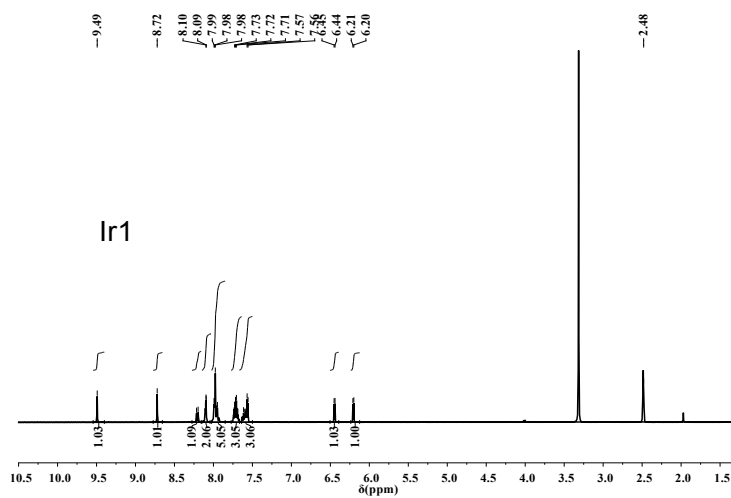


Figure S13. <sup>1</sup>H NMR of Ir1 in DMSO

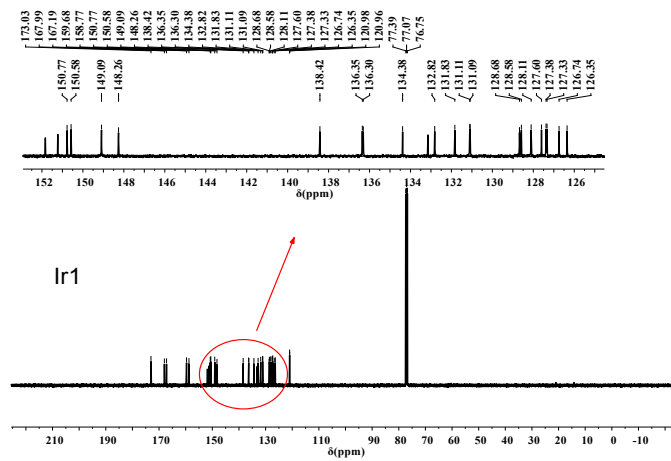


Figure S14.  $^{13}\text{C}$  NMR of Ir1 in  $\text{CDCl}_3$

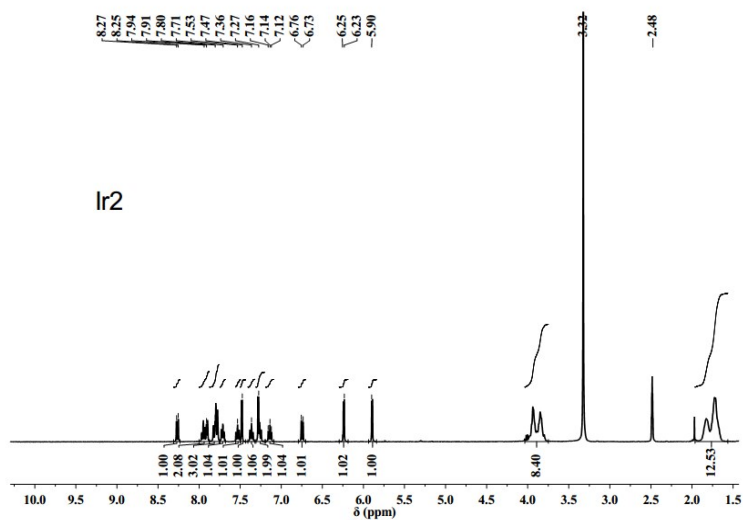


Figure S15.  $^1\text{H}$  NMR of Ir2 in DMSO

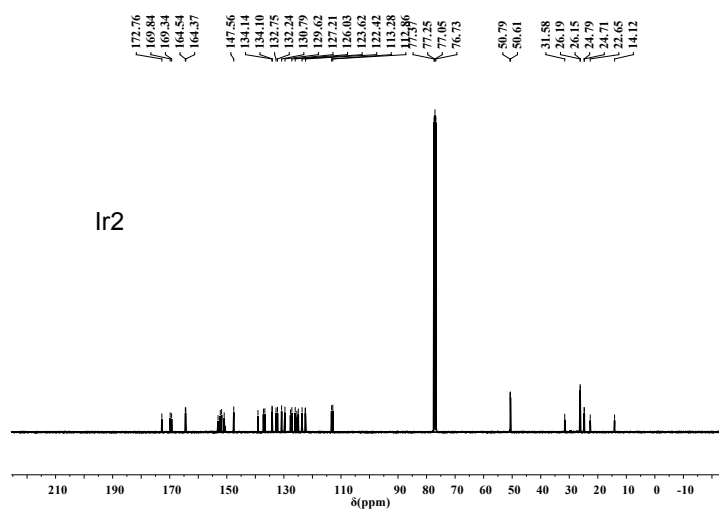


Figure S16.  $^{13}\text{C}$  NMR of Ir2 in  $\text{CDCl}_3$



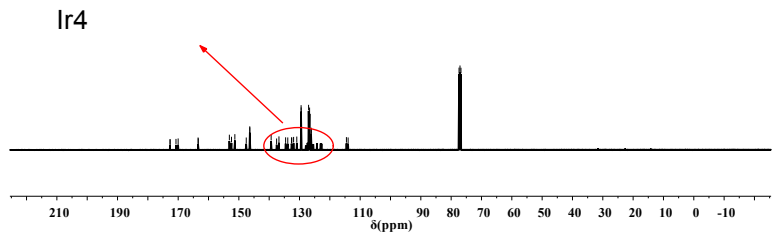
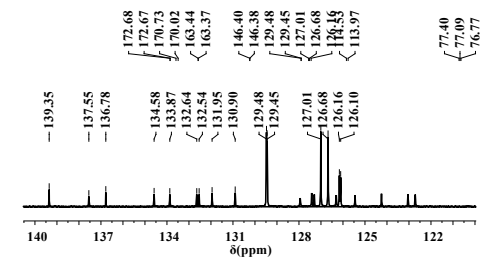
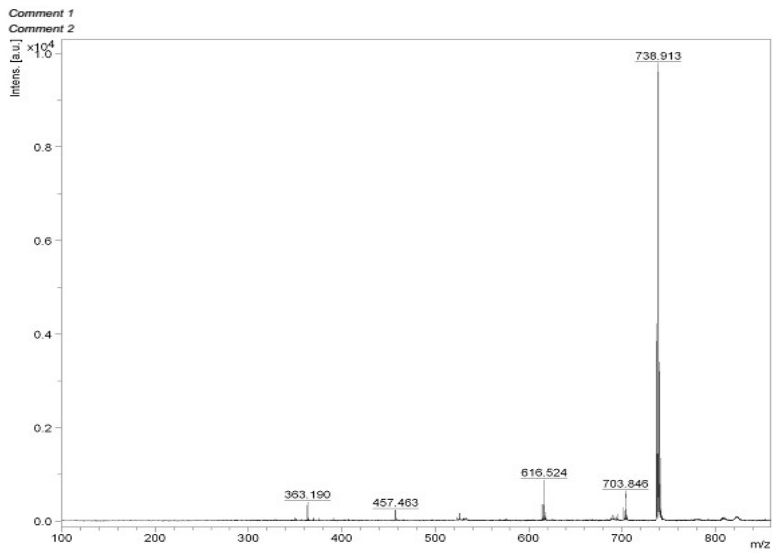
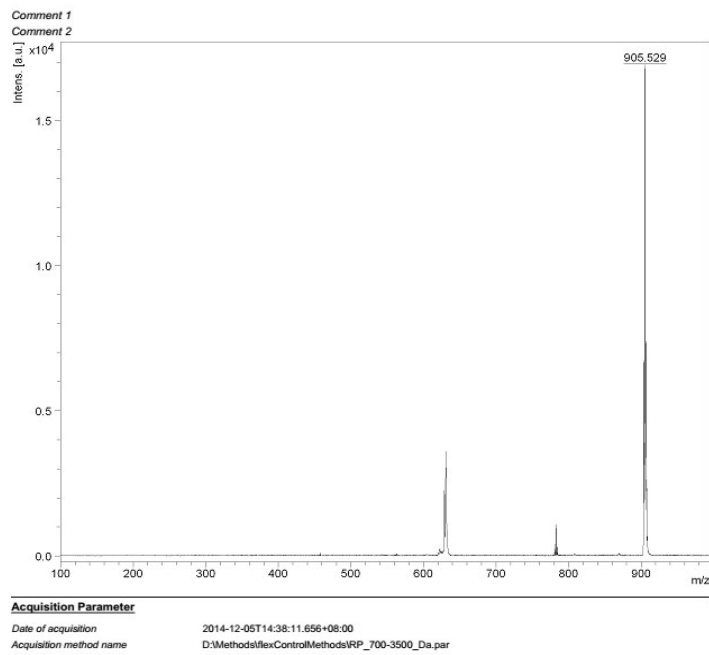


Figure S20.  $^{13}\text{C}$  NMR of Ir4 in  $\text{CDCl}_3$



Acquisition Parameter  
Date of acquisition 2014-12-05T14:40:17.031+08:00  
Acquisition method name D:\Methods\MexControlMethods\RP\_700-3500\_Da.par

Figure S21. MALDI-TOF spectrum of Ir1



**Figure S22.** MALDI-TOF spectrum of Ir2

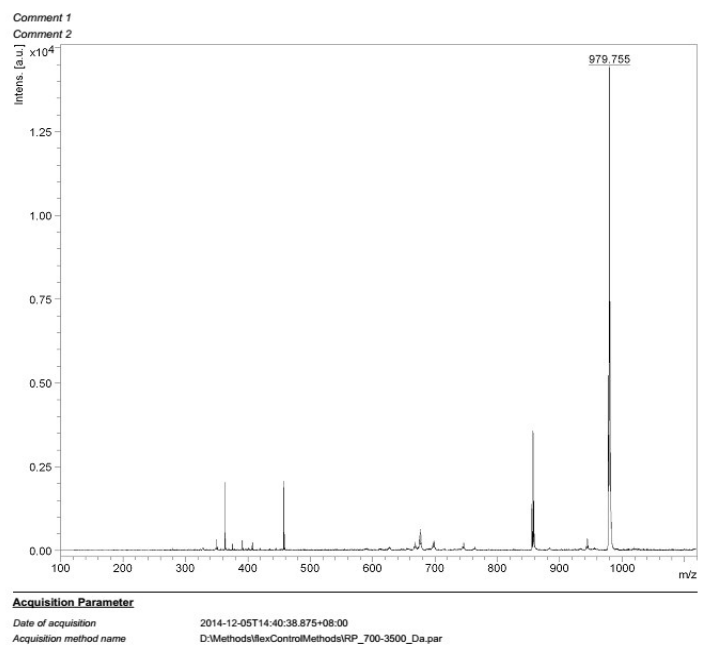


**Figure S23.** MALDI-TOF spectrum of Ir3

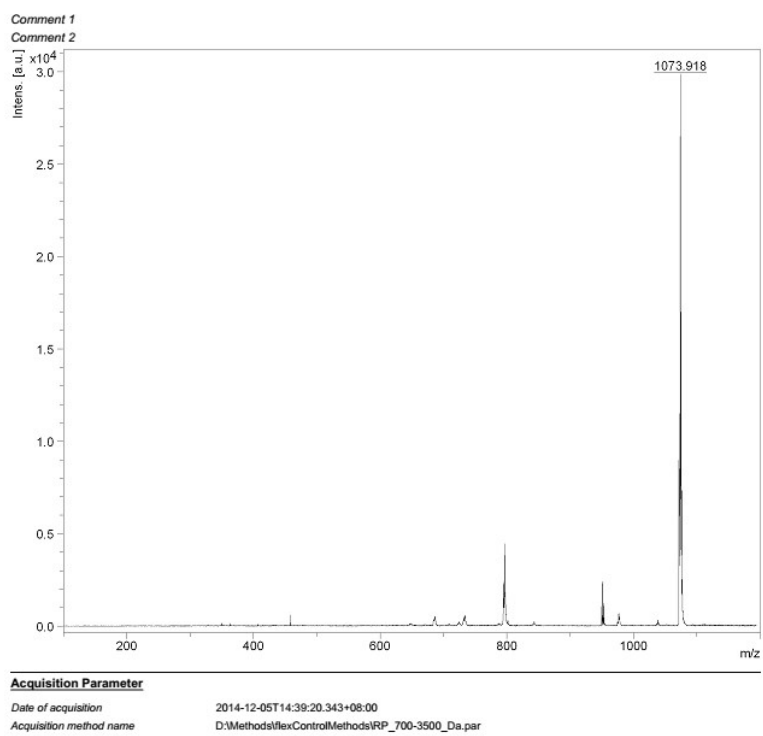


**Figure S24.** MALDI-TOF spectrum of Ir4